Volume 1 | Number 1 | Jan 2013 | Pages 1–100

Journal of
Materials Chemistry A

Materials for energy and sustainability
www.rsc.org/materialsA

Li⁺

ROYAL SOCIETY
OF CHEMISTRY

ROYAL SOCIETY
OF CHEMISTRY

www.rsc.org/materialsA

Journal Name

ARTICLE

Bis(fluoromalonato)borate (BFMB) Anion Based Ionic Liquid As an Additive for Lithium-Ion Battery Electrolytes

Xiao-Guang Sun[a],* Chen Liao[a], Loïc Baggetto[b], Bingkun Guo[a], Raymond R. Unocic[c], Gabriel M. Veith[b], Sheng Dai[a,d]

Propylene carbonate (PC) is a good solvent for lithium ion battery applications due to its low melting point and high dielectric constant. However, PC is easily intercalated into graphite causing it to exfoliate, killing its electrochemical performance. Here we report on the synthesis of a new ionic liquid electrolyte based on partially fluorinated borate anion, 1-butyl-1,2-dimethylimidazolium bis(fluoromalonato)borate (BDMIm.BFMB), which can be used as an additive in 1 M $LiPF_6$/PC electrolyte to suppress graphite exfoliation and improve cycling performance. In addition, both PC and BDMIm.BFMB can be used synergistically as additive to 1.0M $LiPF_6$/methyl isopropyl sulfone (MIPS) to dramatically improve its cycling performance. It is also found that the chemistry nature of the ionic liquids has dramatic effect on their role as additive in PC based electrolyte.

1. Introduction

The choice of solvent and combinations plays a critical role in the cycling performance of battery electrodes such as graphite. The viscosity and dielectric constant of these molecules directly mediate the ionic conductivity of the electrolyte while reactivity of these molecules dictates the formation of the Solid Electrolyte Interphase (SEI) structure. The ultimate goal is to optimize the surface reactivity and bulk transport properties to obtain stable long lasting electrodes. From a conductivity point of view PC is one of the best solvents. It has a low melting point (-49°C) and high dielectric constant ($\varepsilon = 64$). However, PC does not react with the graphite surface to form a stable SEI. Instead, it intercalates within the graphite causing it to exfoliate.[1] As a result, ethylene carbonate (EC) has become an indispensable component in commercial carbonate electrolytes thanks to its uniqueness in passivating graphite electrode. However, EC has a high melting point of 37°C, which limits the low-temperature performance of LIBs, even with the addition of linear carbonates.

To enable the use of PC in graphite based lithium ion batteries many groups have focused on using sacrificial additives such as vinylene carbonate (VC),[2,3] vinyl ethylene carbonate (VEC),[4] fluoroethylene carbonate (FEC),[3] vinyl ethylene sulfite (VES),[3,5] butylene carbonate (BC),[6] and 2-Phenylimidazole [7] to prevent graphite exfoliation. Alternatively, Ogumi et al have shown that high salt concentration such as 2.72 M [8] or higher than 3.27m lithium bis(perfluoroethyl sulfonyl)imide (LiBETI) were needed to stop the PC co-intercalation.[2] However, such high salt concentrations adversely reduced the ionic conductivity for practical applications.[2,8] On the other hand, Abe et al demonstrated that solvents with higher donor numbers such as DMSO and diethoxymethane (DEM) could be added to 1.0M $LiClO_4$/PC electrolyte in high concentrations to

stop PC co-intercalation, which unfortunately resulted in low coulombic efficiency and low intercalation capacity.[9] Recently, it was found that a new lithium salt, lithium bis(oxalate)borate (LiBOB),[10] can effectively stabilize the graphitic structure in pure PC electrolyte without using ''film forming'' additives. [11] This requires the use of 1.0 m LiBOB in PC solution to inhibit graphite exfoliation.[12] Unfortunately, similar to the case of LiBETI that high concentration of LiBOB results in lower ionic conductivity compared with the native 1 m $LiPF_6$/PC electrolyte.[13]

Here we report on the synthesis and application of a new ionic liquid, 1-butyl-2,3-dimethylimidazolium bis(fluoromalonato)borate (BDMIm.BFMB) (Scheme 1) that can effectively passivate the graphite electrode in 1.0M $LiPF_6$/PC electrolyte. Unlike organic additives, ionic liquid[14-16] is non-volatile, non-flammable, which can improve the safety of the organic electrolytes. Also different from LiBOB, the ionic liquid can be used at a much small quantity, typically 2-5 wt%, to suppress graphite exfoliation in the PC-based electrolytes. Furthermore, the combination of PC and ionic liquid can be used as an additive in alky sulfone electrolyte to stabilize its cycling performance with graphite electrode.

2. Experimental

2.1. Synthesis

Methyl isopropyl sulfone (MIPS) was purchased from TCI America Inc. and purified by first heating over calcium hydride at 60 $^\circ$C for overnight, followed by distillation under vacuum and stored over dried molecular sieve inside the glovebox. The moisture content of MIPS is less than 30 ppm as determined by Karl Fisher titration. Diethyl fluoromalonate was purchased from Synnovator, Inc. Boric acid, sodium hydroxide, sodium carbonate, 1-bromobutane, 1-ethylmethylimidazolium chloride, N-methylpyrrolidone (NMP),

polyvinylidene fluoride (PVdF), 1,2-dimethylimidazole, and anhydrous acetonitrile were purchased from Aldrich. Anhydrous propylene carbonate (PC), dimethyl carbonate (DMC), and lithium hexafluorophosphate (LiPF$_6$) were purchased from Novolyte Technologies, Inc. and were used directly for electrolyte formulation. Lithium bis(trifluoromethanesulfonyl)imide (LiTFSI) was purchased from 3M Inc. and that used for electrolyte formulation was dried at 150°C under vacuum for 24hr. Natural graphite and copper foil were bought from TMI corporation.

2.1.1 Synthesis of fluoromalonic acid Sodium fluoromalonate was synthesized using a modified procedure from Horwitz's.[17] Sodium hydroxide (45 g) was dissolved in 250 ml of water followed by dilution with 1000 mL of ethanol. The solution was heated to 60 ^{o}C and diethyl fluoromalonate (100g) was added *via* addition funnel. A white precipitate was formed immediately. The mixture was stirred at 60 ^{o}C for 45 min. The fine white precipitate was collected and dried at 50 ^{o}C under vacuum overnight to get the product in quantitative Yield. ^{1}H NMR (Acetone-d$_6$, 400 MHz) δ PPM: 4.92 (d, 1H, ^{2}J$_{HF}$ = 53.2 Hz).^{13}C NMR (Acetone-d$_6$, 100 MHz) δ PPM: 172.9 (d, ^{2}J$_{CF}$ = 21.2 Hz), 89.75 (d, ^{2}J$_{CF}$ = 185 Hz).

The dried sodium fluoromalonate was dissolved in excess concentrated HCl solution and the heterogeneous solution was stirred at room temperature overnight. The HCl was removed by vigorously bubbling nitrogen, followed by concentrating at 80 ^{o}C on a rotary evaporator. The residual liquid was dissolved in 500 mL ether and the precipitated NaCl was filtered. Fluoromalonic acid was obtained after the solvent was removed on the rotary evaporator. Yield: 90%. ^{1}H NMR (Acetone-d$_6$) δ PPM: 8.47 (s, 2H), 5.82 (d, ^{2}J$_{HF}$ = 48 Hz). ^{13}C NMR (Acetone-d$_6$) δ PPM: 165.2 (d, ^{2}J$_{CF}$ = 24.3 Hz), 84.98 (d, ^{1}J$_{CF}$ = 190.3 Hz)

2.1.2. Synthesis of sodium bis(fluoromalonato)borate (NaBFMB) A modified procedure of Wietelmann's was used.[18] Fluoromalonic acid (10 g) and boric acid (2.54 g) were dissolved in 20 mL of water. Under stirring sodium carbonate (2.17 g) was added slowly and gas bubble was formed. After the gassing was slowed down, the solution was heated to 90 ^{o}C for 0.5 h, followed by removing water on rotary evaporator. The residual solid was transferred into an Ar-filled glove-bag and grounded in a mortar. It was further purified by repeated crystallization from acetonitrile. The salts were dried in a vacuum oven at 100 ^{o}C for 2 days. Yield: 80%. ^{1}H NMR (DMSO-d$_6$) δ PPM: 6.07 (d, ^{2}J$_{HF}$ = 43.6 Hz). ^{11}B NMR (DMSO-d$_6$) δ PPM: -18.18. ^{19}F NMR (DMSO-d$_6$) δ PPM: -64.91 (^{2}J$_{HF}$ = 44.4 Hz). ^{23}Na NMR (DMSO-d$_6$) δ PPM: 0.
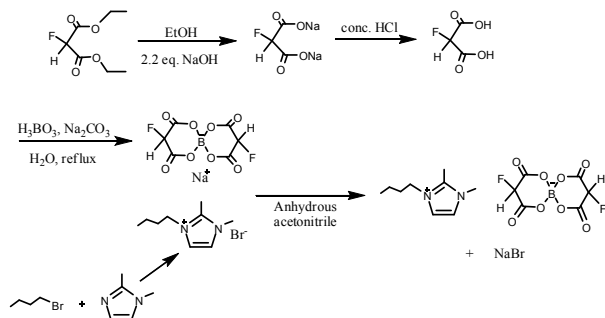
Scheme 1 Synthesis of 1, 2-dimethyl-3-butylimidazolium bis(monofluoromalonato)borate (BDMIm.BFMB).

2.1.3. Synthesis of 1-butyl-2,3-dimethylimidazolium bis(fluoro malonato)borate (BDMIm.BFMB) 1-butyl-2,3-dimethyl imidazolium bromide was synthesized by reacting 1,2-dimethylimidazle with 1-bromobutane following the reported procedure.[19] The imidazolium bromide salt was stirred at room temperature with excess sodium bis(fluoromalonato)borate in anhydrous acetonitrile under argon for 3 days to allow the reaction complete. After reaction, the flask was transfer to an Ar-filled glove-bag and the sodium bromide was filtered off. The solvent in the filtrate was evaporated on a rotary evaporator at reduced pressure. The residue was freeze dried overnight and then dissolved in 20 mL dichloromethane. The solution was allowed to stand at room temperature overnight. After filtration and evaporation of the solvent, the residue solid was further freeze dried and stored in a Glove box. Excellent purity of the resulting orthoborate ionic liquid was confirmed by ^{1}H, ^{11}B, ^{19}F. No peak is present in the ^{23}Na NMR spectrum. Yield: 30%. ^{1}H NMR (DMSO-d$_6$) δ PPM: 7.64-7.66 (m, 2H), 6.063 (d, ^{2}J$_{HF}$ = 45.2 Hz), 4.44 (t, 2H), 4.1 (s, 3H), 2.91 (s, 3H), 2.11-2.16 (m, 2H), 1.72-1.78 (m, 2H), 1.36 (t, 3H). ^{11}B NMR (DMSO-d$_6$) δ PPM: -17.99.^{19}F NMR (DMSO-d$_6$) δ PPM: -66.59 (d, ^{2}J$_{HF}$ = 45.3 Hz). ^{23}Na NMR (DMSO-d$_6$) δ PPM: No peaks. Elemental Analysis: Calculated, C44.58%, H, 4.74%, N 6.93 %; Experimental, C 44.91%, H 4.82%, and N 6.87%.

2.2. Characterization

^{1}H, ^{7}Li, ^{11}B, and ^{19}F NMR spectra were recorded on a Bruker Avance 400 MHz spectrometer. The chemical shifts were reported in ppm relative to tetramethylsilane (TMS) or residual protonated solvent peaks in ^{1}H NMR spectra. LiBF$_4$ in DMSO-d$_6$ was used as an external standard for ^{7}Li, ^{11}B, and ^{19}F NMR spectra. Surface morphology of the cycled electrode was observed using a Hitachi NB5000 dual beam focused ion beam (FIB)/ scanning electron microscope (SEM) instrument. The samples were loaded in an argon filled glovebox and transferred to the instrument under a protective argon environment with a specially designed SEM transfer stage.

Graphite electrode was obtained by casting a well-homogenized slurry of natural graphite (85 wt %), acetylene black (5 wt%), and PVdF (10 wt %) in NMP on copper foil using a doctor blade. After evaporation of the solvent, the electrodes were pressed under a hydrolytic pressure of 1 ton for 1 min before being cut into discs with a diameter of 13 mm and further dried at 110°C for 24 h. They were then transferred into a glovebox for cell assembly. Coin cells were assembled inside the glovebox by using a graphite electrode as the cathode, lithium metal as the anode, Celgard 3401 as the separator, and 1.0M LiPF$_6$/PC and 1.0M LiPF$_6$/MiPS with or without BDMIm.BFMB as the electrolytes. The cells were cycled on an Arbin BT2000 cycling station under different current densities between 0.005 and 3.0 V at room temperature. Cyclic voltammetry (CV) was performed by using graphite as the working electrode and lithium disc as both the counter and the reference electrodes on a Gamry Instrument under the scan rate of 1.0 mV s^{-1}.

Surface chemistry was probed using a PHI 3056 XPS spectrometer with Al K$_α$ source (1486.6 eV) in a cryo-pumped vacuum chamber with a pressure below 10^{-8}Torr. Samples were dissembled inside an Ar filled glovebox, rinsed with anhydrous DMC and transferred to the XPS chamber using an air-tight vacuum transfer system. High resolution scans were taken at 350 W with 23.5 eV pass energy, 0.05 eV energy step and from 30 to 120 repeats to improve the signal to noise ratio. Survey scans were measured at 350 W with 93.9 eV pass energy, 0.5 eV energy step and 10 repeats.

The binding energies were shifted by setting the aliphatic carbon signal to 284.8 eV to account for charging. The intensities of the presented spectra are not normalized and are simply shifted vertically for clarity. Surface concentrations are calculated by integrating the peaks area and using standard atomic sensitivity factors supplied by the equipment manufacturer. Assignments indicated in the figures are based on fitting the data using Gaussian-Lorentzian functions and a Shirley-type background.

3. Results and discussion

3.1 BDMIm.BFMB as an additive in 1.0M LiPF$_6$/PC electrolyte

Fig. 1 shows cyclic voltammetry of 1 M LiPF$_6$/PC, with and without BDMIm.BFMB as additive on a graphite working electrode at a scan rate of 1 mV s^{-1}. As expected, the absence of additive results in a pronounced reduction peak around 1 V, which is consistent with graphite exfoliation (Fig. 1a).[20] With 2 wt% IL as additive, there is a small reduction peak around 1.5 V, followed by a large reduction peak below 0.5 V (Fig. 1b). The peak at 1.5V increases with the amount of BDMIm.BFMB (Fig. 1c), confirming that they are related to the reduction of BDMIm.BFMB. The peak around 0.5 V is attributed to the co-intercalation and reduction of PC, which is disappeared after the first cycle (Fig.1b and 1c). More importantly, the cathodic peak below 0.15 V and the anodic peak between 0.2-0.6 V are the typical peaks corresponding to the lithium intercalation into and de-intercalation from the graphite electrode, respectively. The disappearance of the reduction peaks from both PC and BDMIm.BFMB in the second cycle and the increase of the current densities for the intercalation/de-intercalation with scan numbers indicate that effective solid electrolyte interphase (SEI) was formed on the graphite surface in both solutions (Fig.1b and 1b).
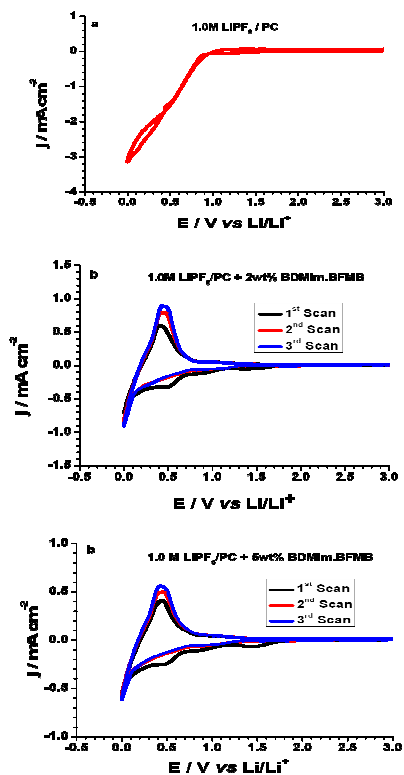

Fig. 1. Cyclic voltammetry of 1.0M LiPF$_6$/PC without (a) and with 2 wt% (b) and 5 wt% % (c) of DMBIm.MFMB at a scan rate of 1mV/s on a graphite working electrode with Li metal as both counter and reference electrode.

For NG∥Li half-cell test, 5 wt% BDMIm.BFMB was used as additive to ensure better cell performance. The addition of 5wt% BDMIm.BFMB is roughly equivalent to the addition of 1 wt% VC,
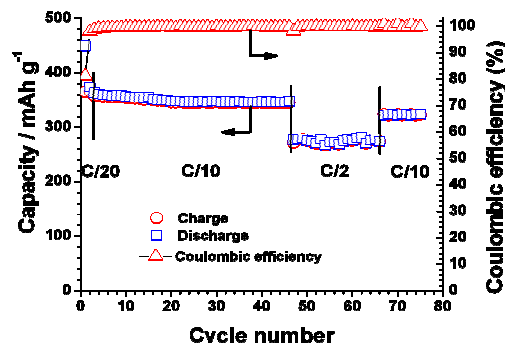

Fig. 2. Charge/discharge capacities and coulombic efficiency of NG∥Li half-cell using 1.0M LiPF$_6$/PC containing 5wt % BDMIm.BFMB under different current rates at room temperature.

considering the molecular weight of the former is 404 g mol^{-1} while that of the latter is only 86 g mol^{-1}. Fig. 2 shows the charge/discharge capacities and coulombic efficiency of the cell under different current rates. During the first two formation cycles at a current rate of C/20, the reversible capacity is around 364 mAh g^{-1}. Once the formation cycles are finished, the current is increased to C/10 and the cell exhibits good cycling performance, i.e. the reversible capacity is still maintained at 346 mAh g^{-1} after 45 cycles. The electrolyte formulation not only supports good cycling performance but also exhibits good rate capability. As shown in Fig.2, when the current rate is further increased to C/2, the reversible capacity is slightly decreased to 275 mAh g^{-1}; once the current rate is reduced back to C/10 after another 20 cycles, the reversible capacity is recovered to 325mAh g^{-1}. The above results show that 5wt% BDMIm.BFMB is indeed enough to forming a stable SEI to suppress the graphite exfoliation in pure PC based electrolyte and maintain good cycling performance.

3.2. BDMIm.BFMB as an additive in 1.0M LiPF$_6$/MIPS electrolyte

The effectiveness of BDMIm.BFMB as an additive in 1.0M LiPF$_6$/PC electrolyte inspires us to investigate its use in alkyl sulfone electrolytes,[21-23] which usually have poor compatibility with graphite electrode and rely additives such as VC to exhibit good cycling performance.[24] Here, methyl isopropyl sulfone (MIPS) was used as a typical solvent in which 1 M LiPF$_6$ was dissolved as the electrolyte. Since MIPS does not like PC that can cause the exfoliation of graphite electrode, several scenarios were tested and compared, i.e. both BDMIm.BFMB and PC were used separately and collectively as additives to the 1.0 M LiPF$_6$/MIPS electrolyte. For the pure sulfone electrolyte, there is small reduction peak at 1.3V followed by a broad one at 0.4V (Fig. 3a). The former peak can be attributed to the bulk reduction of MIPS while the latter is attributed to the co-intercalation and reduction of the MIPS, all of which disappear after the first cycle. With 5wt% BDMIm.BFMB is used as additive (Fig.3b), besides the above typical reduction peaks related to MIPS there is one broad reduction peak of BDMIm.BFMB between 1.5-2.0V, similar to that observed in Fig.1b and c. When 10wt% PC is used as additive, there is a giant reduction peak between 0.4-0.8V, apparently due to the co-intercalation and reduction of PC (Fig.3c). The double peak character, however, indicates that there is also contribution from the co-intercalation and reduction of MIPS, as
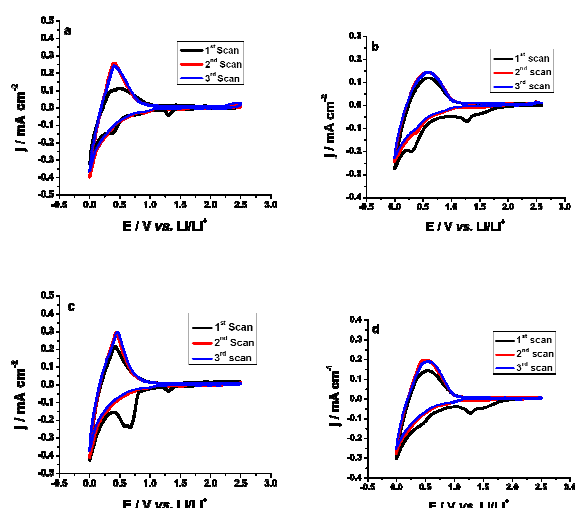
Fig. 3. Cyclic voltammetry of a) 1.0M LiPF$_6$/MiPS and that with b) 5wt% BDMIm.BFMB; c) 10wt% PC and d) 10wt% PC + 5wt% BDMIm.BFMB on a graphite working electrode with Li metal as both counter and reference electrode at a scan rate of 1mV/s.

observed in pure sulfone electrolyte and that with 5wt% BDMIm,BFMB. Once 10wt% PC and 5wt% BDMIm.BFMB are used together as additives, the reduction peaks due to the co-intercalation of MIPS and PC are significantly reduced (Fig.3d).

If simply judged from the CVs of the four electrolyte formulations such as the disappearance of the reduction peaks after the first scan and the increase of current densities with the scan cycles (Fig. 3), it would suggest that somehow the graphite electrode surface was passivated and should support good cell cycling. However, unlike the exfoliation in PC electrolyte, the CVs are not well aligned with the cycling performance for the sulfone electrolyte. Fig.4 shows the cycling performance of the cells using the four electrolyte formulations under a current rate of C/10. For the pure sulfone electrolyte, the initial charge (lithium de-intercalation) capacity is only 84 mAh g^{-1} with a coulombic efficiency of 46.2%, and the cell decades quickly with cycling (Fig.4a). With the addition of 5 wt% BDMIm.BFMB, the initial charge capacity increases to 100 mAh g^{-1} with a coulombic efficiency of 59.5%. However, unlike the PC based electrolyte, 5wt% BDMIm.BFMB alone cannot prevent the capacity fading for the sulfone electrolyte; even it has a nominal better cycling performance than the pure sulfone electrolyte (Fig.4a). When 10 wt% PC is used alone as the additive, the initial charge capacity is jumped to 207 mAh g^{-1} with a high coulombic efficiency of 74.5%. In addition, the cycling stability is significantly improved, that is, the reversible capacity slowly decreases to 176 mAh g^{-1} after 40 cycles (Fig.4b). With both 10wt% PC and 5 wt% BDMIm.BFMB as the additives, the initial discharge and charge capacities are increased to 323 and 275 mAh g^{-1}, respectively, resulting in a much higher coulombic efficiency of 85.1% (Fig.4b). Also, the cycling performance is significantly improved, for example, the reversible capacity is still as high as 263 mAh g^{-1} after 40 cycles. Furthermore, the coulombic efficiency is immediately increased to 99% after the first two cycles. As a contrast, for the cell using 10wt% PC as additive the coulombic efficiency is slowly increasing and it takes 25 cycles to reach above 99% (Fig.4b). The above results suggest that there is a synergistic effect of PC and BDMIm.BFMB on SEI formation and cell performance.

3.3 Surface characterization of cycled graphite electrodes

The cycled half-cells were dissembled inside an Argon filled glovebox and washed three times with dry dimethyl carbonate (DMC) and two times with dry dichloromethane, followed by drying under vacuum. An air protection SEM transfer system was used to transport the specimens to the scanning electron microscope (SEM) for characterization. Representative SEM images of the surface structure are presented in Fig.5 in low and high magnification images. For comparison a low magnification image of the un-cycled graphite electrode is presented in Fig.5a. It was noticed during electrode washing that the one cycled in pure PC electrolyte (Fig.5b) was delaminated from the current collector and broken into small pieces. Examination of the surface structure shows that the individual graphite electrodes are no longer present; rather a thick film is which can be explained by co-intercalation of PC and exfoliation of graphite, which leaves behind a composite structure of exfoliated graphite and electrolyte decomposition products. As a contrast, the electrode cycled in PC+ 5wt% BDMIm.BFMB (Fig. 5c) shows clearly that the graphite particles are still intact, and that the surface is covered with SEI product. When cycled in the pure sulfone electrolyte (Fig.5d) the graphite electrodes are still intact; however, the graphite is covered with a thick SEI film containing numerous microcracks. The electrode cycled in MIPS + 5wt% BDMIm.BFMB (Fig.5e) and that cycled in MIP +10 wt% PC (Fig.
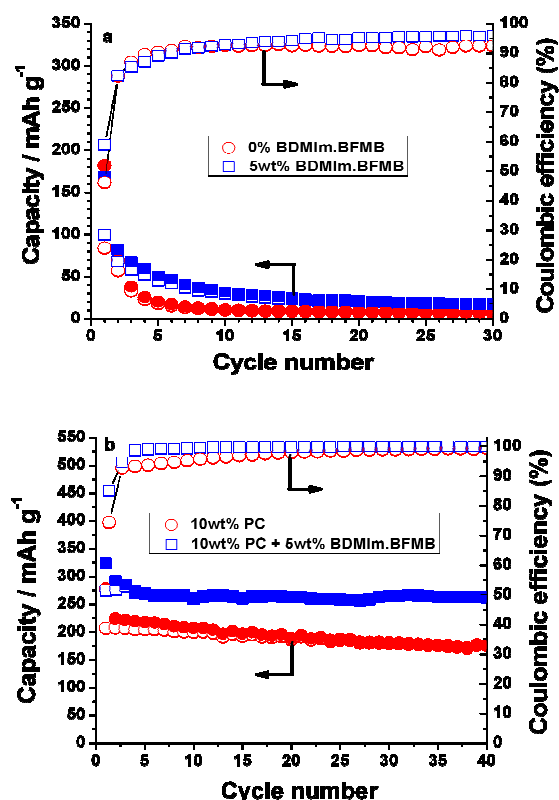

Fig.4. Discharge/charge capacities and coulombic efficiency of NG∥Li half-cell using 1.0M LiPF$_6$/MIPS containing a) without and with 5wt% BDMIm.BFMB and b) with 10 wt% PC and with both 10wt% PC and 5wt% BDMIm.BFMB as additive under the current rate of C/10 (filled symbols for discharge capacity and open symbols for charge capacity).

5f) are covered with thick SEI films. One big difference between these two electrode morphologies is the large cracks observed in the electrode cycled in MIPS+5wt% BDMIm.BFMB electrolyte, which is hypothesized to be the cause for the difference in their cell cycling performance (Fig.4a and b). Finally, the electrode cycled in MIPS+10wt% PC+5wt% BDMIm.BFMB (Fig. 5g) is still intact and the individual graphite electrode particle surface is covered with a thick SEI layer. Generally, the cells failed in cycling performance are either due to too thick SEI layer (Fig. 5b) or due to large surface cracks (Fig. 5d and e) while the cells with good cycling are due to well-formed SEI layer with intact graphite electrodes (Fig.5c and g). Also, comparatively the electrodes cycled in MIPS based electrolytes are covered thicker SEI layers than that cycled in PC based electrolytes.
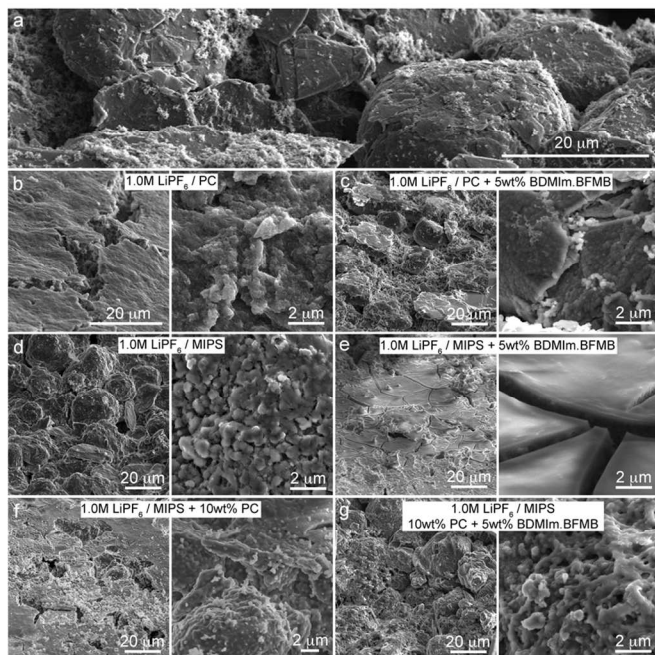

Fig. 5. SEM images of the surface morphology of a) pristine graphite electrode and cycled graphite electrodes in b) 1.0M LiPF$_6$ / PC; c) 1.0M LiPF$_6$ / PC + 5wt% BDMIm.BFMB; (d) 1.0M LiPF$_6$ / MIPS; e) 1.0M LiPF$_6$ / MIPS + 5wt% BDMBIm.BFMB; f) 1.0M LiPF$_6$ / MIPS + 10wt% PC; g) 1.0M LiPF$_6$ / MIPS + 10wt% PC + 5wt% BDMIm.BFMB.
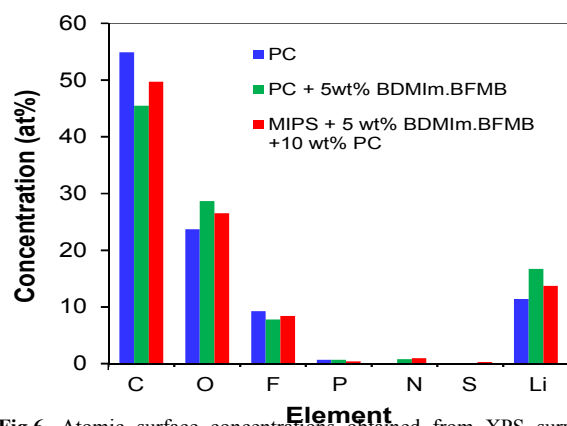

Fig.6. Atomic surface concentrations obtained from XPS survey scans for the various NG electrodes cycled in 1.0M LiPF$_6$/PC (blue), 1.0M LiPF$_6$/PC + 5wt% BDMIm.BFMB (green) and 1.0M LiPF$_6$/MIPS + 5wt% BDMIm.BFMB + 10wt% PC (red).

To further elucidate the additive effect on SEI formation, some of the cycled graphite electrodes were also surveyed using XPS. Fig. 6 shows the atomic concentrations measured on the surfaces of the electrodes cycled in 1.0M LiPF$_6$/PC, 1.0M LiPF$_6$/PC + 5wt% BDMIM.BFMB, and 1.0M LiPF$_6$/MIPS + 10wt% PC + 5wt% BDMMB.BFMB. Due to an overlap of B1s with P2s, the concentration of B cannot be calculated. As shown in Fig.6, the electrode cycled in pure PC electrolyte has a larger amount of C (54.9 at%), less O (23.7 at%), about the same quantity of F (9.3 at%) and P (0.7 at%), and less Li (11.4 at%). The addition of 5wt% BDMIm.BFMB to PC electrolyte or the use of 5wt% BDMIm.BFMB and 10wt% PC in MIPS electrolyte yields, oppositely, relatively less C (45.5 and 49.7 at%), more O (28.7 and 26.5 at%), slightly less F (7.8 and 8.4 at%), similar P (0.7 and 0.4 at%), a small amount of N (0.8 and 1.0), traces of S (0.0 and 0.3 at%), and larger quantities of Li (16.7 and 13.7 at%). These differences in chemical compositions are closely related to the used electrolytes and additives. For pure PC electrolyte, lower quantities of carbonates (CO$_3^{2-}$) such as lithium alkyl carbonates (RCO$_2$Li) or lithium carbonates (Li$_2$CO$_3$), species with O-C=O groups such as carboxylates or esters, and ethers such as poly alkyl ethers, lithium alkoxides (LiOR) are present. In addition, the increase in C is related to higher amounts of aliphatic carbon (284.8 eV) and species at 282.8 eV (Fig.7). The latter were also reported in previous reports for charged graphite electrodes in LiBOB based electrolyte and may be due to differential charging or reduced C species. [25] When cycling in PC + 5wt% BDMIm.BFMB or MIPS + 10wt%PC + 5wt% BDMIm.BFMB electrolyte, the contributions of the organic species are much higher, especially the O-C=O groups in MIPS + 10wt% PC + 5wt% BDMIm.BFMB electrolyte.
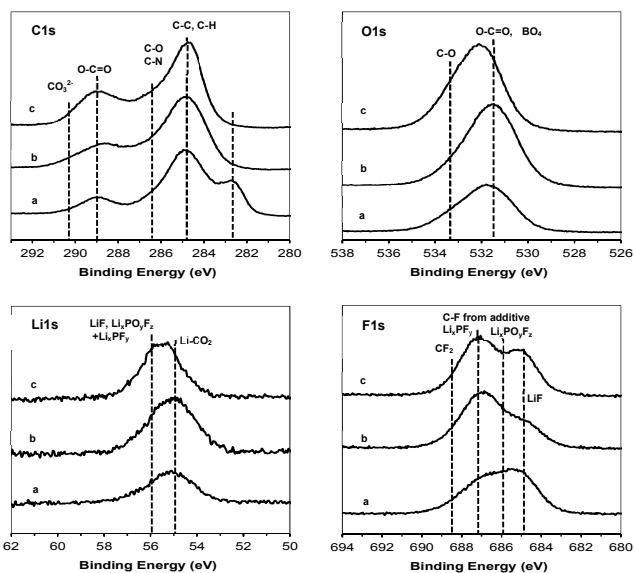

Fig. 7. C1s, O1s, Li1s and F1s high resolution XPS spectra collected on cycled NG electrodes in a) 1.0M LiPF$_6$/PC, b) 1.0M LiPF$_6$/PC+5wt% BDMIm.BFMB and c) 1.0M LiPF$_6$/MIPS+5wt% BDMIm.BFMB +10wt% PC.

Apart from above organic species, inorganic species are well evidenced in the P2p, Li1s and F1s spectra, particularly LiF, Li$_x$PF$_y$ and 'Li$_x$PO$_y$F$_z$' (LiF + P$_2$O$_5$ or Li$_x$POF$_3$) compounds, which are typical decomposition products of the LiPF$_6$ salt. [26] The addition of 5wt% BDMIm.BFMB to PC electrolyte seems to decrease the proportion of LiF (685 eV in F1s) in favour of Li$_x$PO$_y$F$_z$ and Li$_x$PF$_z$ (686-687 eV in F1s) species, but to a lesser extent when using the

MIPS + 10wt% PC + 5wt% BDMIm.BFMB electrolyte. There is also an increase in the relative quantity of Li_xPF_y over $Li_xPO_yF_z$ for the use of PC + 5wt% BDMIm.BFMB and MIPS + 10wt% PC + 5wt% BDMIm.BFMB as compared to pure PC electrolyte, as supported by both F1s (**Fig.7**) and P2p (**Fig. 8**) spectra. In addition, the presence of C-F functionalities resulting from the BDMIm.BFMB is expected in F1s at an energy of about 687 eV based on the measurement of the starting BDMIm.BFMB. For all electrodes the signals attributed to PVDF (286.5 and 291 eV in C1s and 688.5 eV in F1s) are not visible, which evidences that the SEI layer is thicker than the typical depth of 5 nm probed by XPS, consistent with the SEM data (Fig.5).
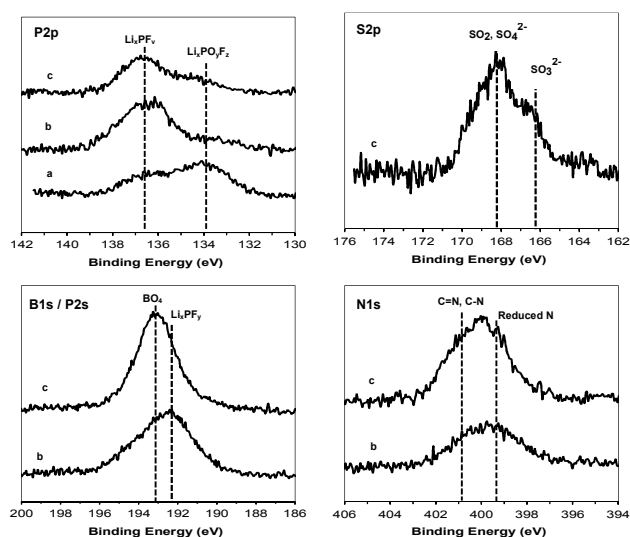

Fig. 8. P2p, S2p, B1s/P2s and N1s high resolution XPS spectra collected on cycled NG electrodes in a) 1.0M $LiPF_6$/PC, b) 1.0M $LiPF_6$/PC+5wt% BDMIm.BFMB and c) 1.0M $LiPF_6$/MIPS+5wt% BDMIm.BFMB +10wt% PC.

Although B1s core level partly overlaps with P2s, based on the P2p signals measured for the aforementioned P-containing species, P species in P2s are expected at lower energies than BO_4 groups at ~193eV in B1s (**Fig.8**). The lower amount of P found in the P2s spectrum of the electrode cycled in MIPS + 5wt% BDMIm.BFMB + 10wt% PC is consistent with the P2p spectra used for the quantification, which is 0.4 at% and 0.7 at% for the electrode cycled in MIPS+5wt% BDMIm.BFMB + 10wt% PC and PC + 5wt%
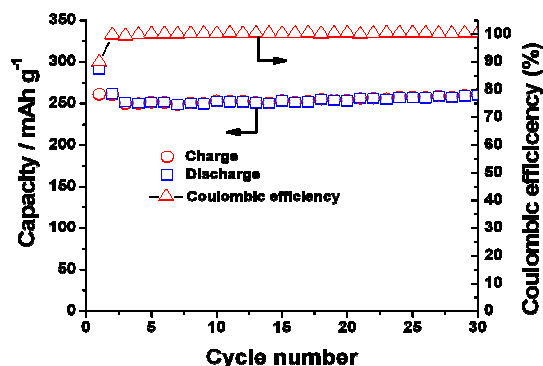

Fig. 9. a) Charge/discharge capacities and coulombic efficiency of NG‖Li half-cell cycled in 1.0M $LiPF_6$ containing 5wt% BDMIm.TFSI under a current rate of C/10.

BDMIm.BFMB, respectively. Moreover, the binding energy of the borate groups at ~193 eV for the cycled electrode is the same as that of starting BDMIm.BFMB compound (not shown) and that of $LiBFMB$,[27] suggesting that these groups do not undergo electrochemical reactions. In contrast, the N species in BDMIM.BFMB measured at 401 eV (not presented) are partly reduced into species with a binding energy of ~399 eV (**Fig.8**). The use of MIPS also induces the presence of S-containing species, with energies typical of sulfites (SO_3^{2-}, ~166eV) and sulfone or sulfates (SO_2, SO_4^{2-}, ~168eV). The lower binding energy is indicative of reduced sulfone species, suggesting that MIPS is electrochemically reduced into species like sulfites (SO_3^{2-}) or hyposulfites (SO_2^{2-}); nevertheless the total amount S present on the electrode surface is fairly small (0.3 at%).
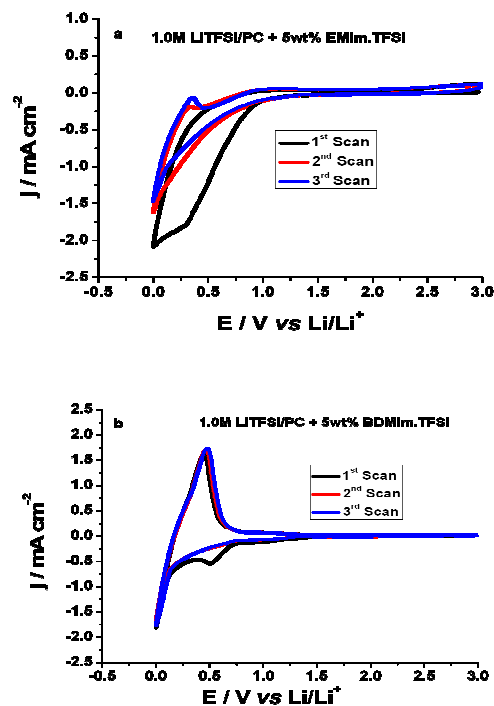

Fig.10. Cyclic voltammetry of 1.0M LiTFSI/PC containing 5wt% a) EMIm.TFSI and b) BDMIm.TFSI on a graphite working electrode at a scan rate of 1mV/s with Li metal as both counter and reference electrode.

3.4 The role of BFMB anion in SEI formation

The XPS result that B species from the cycled electrode are the same as that from the starting material suggests that the anion is not reduced. Instead, it might be mainly the cation contributing to the effective SEI formation to prevent graphite exfoliation in PC based electrolyte. To check this hypothesis we have synthesized 1-butyl-2,3-dimethylimidazolium bis(trifluoro methanesulfonyl)imide (BDMIm.TFSI) according to previously reported procedure and used it as an additive.[19,28,29] As clearly shown in Fig.9, addition of 5wt% BDMIM.TFSI to 1.0M $LiPF_6$/PC produces NG‖Li half-cell with good cycling performance at the cost of a small amount of reversible capacity compared to that measured with 5wt% BDMIm.BFMB shown in Fig. 2. Nonetheless, this result is significantly different from that reported by Zheng et al. that it needs at least 60 vol% of trimethylhexyl ammonium bis(trifluoro methanesulfonyl)imide (TMHA.TFSI) as co-solvent in 1.0M LiTFSI/PC electrolyte to

stop graphite exfoliation.[27] The dramatic difference indicates that the cation structure might be the main cause. To check this we have further synthesized ethylmethylimidazolium bis(trifluoromethane sulfonyl) imide (EMIM.TFSI)[19] and used it as an additive in 1.0M LiTFSI/PC electrolyte, which is same as that used by Zheng et al.[27] Fig. 10a and b show the CVs of 1.0M LiTFSI/PC containing 5wt% of EMIM.TFSI and BDMIm.TFSI, respectively. With 5wt% EMIM.TFSI as additive, there is only one major reduction peak that can be attributed mainly to PC co-intercalation and decomposition as observed for pure PC electrolyte in Fig.1a and also partially to the co-intercalation and decomposition of the EMIm cation.[30] Even after three successive CV scans, there is only a small discernable lithium de-intercalation peak (Fig.10a), and as expected the electrolyte does not support reversible cell cycling (not shown). As a contrast, with 5wt% BDMIm.TFSI as additive, the PC co-intercalation and decomposition is significantly reduced and successful lithium intercalation and de-intercalation are observed. The aforementioned results confirm that indeed the cation structure of the ionic liquids plays a key role in preventing PC co-intercalation and graphite exfoliation.

It is noticed that the reduction peak observed at 1.5V for the electrolyte with BDMIm.BFMB as additive (Fig.1b and c) is not present in the electrolyte with BDMIM.TFSI as additive (Fig.10b), confirming that the reduction peak at 1.5V is specifically attributed to the BFMB anion. Also, the apparent reduction peak between 0.7 and 1.2V in Fig. 1b and c and that discernable one in the same voltage range in Fig 10b are clearly due to the BDMIm cation. These facts confirm that both BDMIm cation and BFMB anion participate in the SEI formation. It is clear that 5wt% of BDMIm.BFMB or BDMIm.TFSI is not enough to weaken the interaction between Li^+ and PC and prevent the co-intercalation of PC as suggested by Zheng et al,[27] but rather it is due to the passivation of the graphite surface by the reduction of BDMIM.BFMB or BDMIm.TFSI that prevents the PC from co-intercalating and exfoliation of the graphite electrode. This is supported by the CVs of the electrolytes based on PC and bis(fluorosulfonyl)imide (FSI) based ionic liquids, which have been actively studied and shown to be compatible with graphite electrodes.[30-33] No lithium intercalation was observed in 0.8M LiTFSI/EMIM.TFSI electrolyte but indeed in 0.8M LiTFSI/EMIm.FSI electrolyte.[30] However, with addition of 10wt% PC to 0.8M LiTFSI/EMIm.FSI electrolyte, one big characteristic peak due to PC co-intercalation and decomposition was observed. Clearly, PC preferred to solvate Li^+ rather than EMIm even though there was only 10wt% PC but large excess EMIm.

It should be emphasized that even though the PC co-intercalation and graphite exfoliation is prevented with the use of BDMIm.BFMB as additive, PC unavoidably participates in the SEI formation on the graphite surface. This is especially true for the case of MIPS based electrolyte. With 10wt% PC alone as additive to the MIPS electrolyte there is an apparent PC co-intercalation peak, which almost disappears after further addition of BDMIm.BFMB (Fig.3c and d). In addition, the low amount of S and high amount of O-C=O groups in the cycled electrode using MIPS + 5wt% BDMIm.BFMB + 10wt% PC, coupled with the good cycling data in Fig. 4 confirm that there is a synergistic effect of BDMIM.BFMB and PC in forming effective SEI and improving cycling stability, which is unattainable through the contribution from the individual components.

Above all, the discrepancy between CVs and XPS regarding the role of BFMB anion in SEI formation can be rationalized as following: the anions reduced in the first two formation cycles are

covered the innermost of the SEI layer where XPS cannot penetrate to pick the B1s signal from those reduced species due to the thick SEI layers formed on the graphite electrodes (Fig.5). On the other hand, the residual BDMIm.BFMB in the electrolyte solution can be exchanged with $LiPF_6$ to form LiBFMB, which has high solubility in high dielectric constant solvents such as PC but no solubility in low dielectric constant solvents such as DMC. [27]

$$BDMIm.BFMB + LiPF_6 \leftrightarrow BDMIm.PF_6 + LiBFMB$$
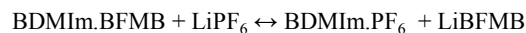
Therefore, the trace amount of LiBFMB left on the top of the graphite electrode after cell disassembling cannot be washed away by both DMC and dichloromethane, resulting in the measured B1s signal being same as that of the starting material.

Conclusions

In summary, we have shown that the newly developed ionic liquid, DMBIm.BFMB, can be used as an additive in pure PC based electrolyte and substantially improve its compatibility with graphite electrode and cycling stability. It is also shown that the chemistry nature of the ionic liquid has a dramatic influence on its function as additive in PC based electrolyte. Furthermore, both PC and DMBIm.BFMB can be used as additive collectively in MIPS based electrolyte to dramatically improve its cycling performance. The safe nature of ionic liquid and low temperature range of PC make the combination useful for lithium ion batteries.

## Acknowledgements

Notes and references

[a]Chemical Sciences Division, Oak Ridge National Laboratory, One Bethel Valley Road, Oak Ridge, TN 37831.
Fax: 1 865 576 5235; Tel: Tel: 1 865 241 8822; E-mail: sunx@ornl.gov
[b]Materials Science and Technology Division, Oak Ridge National Laboratory, One Bethel Valley Road, Oak Ridge, TN 37831.
[c]Center for Nanophase Materials Sciences, Oak Ridge National Laboratory, One Bethel Valley Road, Oak Ridge, TN 37831.
[d]Department of Chemistry, University of Tennessee, Knoxville, TN 37996

(1) Xu, K.: Nonaqueous Liquid Electrolytes for Lithium-Based Rechargeable Batteries. *Chem. Rev.* **2004**, *104*, 4303-4417.
(2) Jeong, S. K.; Inaba, M.; Iriyama, Y.; Abe, T.; Ogumi, Z.: Interfacial reactions between graphite electrodes and propylene carbonate-based solutions: Electrolyte-concentration dependence of electrochemical lithium intercalation reaction. *Journal of Power Sources* **2008**, *175*, 540-546.
(3) Jeong, S. K.; Inaba, M.; Mogi, R.; Iriyama, Y.; Abe, T.; Ogumi, Z.: Surface Film Formation on a Graphite Negative Electrode in Lithium-Ion Batteries: Atomic Force Microscopy Study on the Effects of Film-Forming Additives in Propylene Carbonate Solutions. *Langmuir* **2001**, *17*, 8281-8286.
(4) Hu, Y. S.; Kong, W. H.; Wang, Z. X.; Li, H.; Huang, X. J.; Chen, L. Q.: Effect of morphology and current density on the electrochemical behavior of graphite electrodes in PC-based electrolyte containing VEC additive. *Electrochemical and Solid State Letters* **2004**, *7*, A442-A446.
(5) Zhang, S. S.: A review on electrolyte additives for lithium-ion batteries. *Journal of Power Sources* **2006**, *162*, 1379-1394.

(6)   Chen, R. J.; Wu, F.; Li, L.; Guanb, Y. B.; Qiu, X. P.; Chen, S.; Li, Y. J.; Wu, S. X.: Butylene sulfite as a film-forming additive to propylene carbonate-based electrolytes for lithium ion batteries. *Journal of Power Sources* **2007**, *172*, 395-403.

(7)   Park, G.; Nakamura, H.; Lee, Y.; Yoshio, M.: The important role of additives for improved lithium ion battery safety. *Journal of Power Sources* **2009**, *189*, 602-606.

(8)   Jeong, S. K.; Inaba, M.; Iriyama, Y.; Abe, T.; Ogumi, Z.: Electrpchemcial intercalation of   lithium ion within graphite from propylene carbonate solutions. *Electrochemical and Solid State Letters* **2003**, *6*, A13-A15.

(9)   Abe, T.; Mizutani, Y.; Kawabata, N.; Inaba, M.; Ogumi, Z.: Effect of co-intercalated organic solvents in graphite on electrochemical Li intercalation. *Synthetic Metals* **2002**, *125*, 249-253.

(10)   Xu, W.; Angell, C. A.: LiBOB and its derivatives - Weakly coordinating anions, and the exceptional conductivity of their nonaqueous solutions. *Electrochemical and Solid State Letters* **2001**, *4*, E1-E4.

(11)   Xu, K.; Zhang, S. S.; Jow, T. R.: Formation of the Graphite/Electrolyte Interface by Lithium Bis(oxalato)borate. *Electrochemical and Solid-State Letters* **2003**, *6*, A117-A120.

(12)   Xu, K.; Zhang, S. S.; Poese, B. A.; Jow, T. R.: Lithium Bis(oxalato)borate Stabilizes Graphite Anode in Propylene Carbonate. *Electrochem. and Solid-State Letters* **2002**, *5* A259-A262

(13)   Ding, M. S.; Xu, K.; Jow, T. R.: Conductivity and Viscosity of PC-DEC and PC-EC Solutions of LiBOB. *Journal of the Electrochemical Society* **2005**, *152*, A132-A140.

(14)   Armand, M.; Endres, F.; MacFarlane, D. R.; Ohno, H.; Scrosati, B.: Ionic-liquid materials for the electrochemical challenges of the future. *Nat Mater* **2009**, *8*, 621-629.

(15)   Sun, X. G.; Dai, S.: Electrochemical investigations of ionic liquids with vinylene carbonate for applications in rechargeable lithium ion batteries. *Electrochimica Acta* **2010**, *55*, 4618-4626.

(16)   Gerbaldi, C.; Nair, J. R.; Ahmad, S.; Meligrana, G.; Bongiovanni, R.; Bodoardo, S.; Penazzi, N.: UV-cured polymer electrolytes encompassing hydrophobic room temperature ionic liquid for lithium batteries. *Journal of Power Sources* **2010**, *195*, 1706-1713.

(17)   Horwitz, C. P.; Ghosh, A.: Synthesis of Macrocyclic Tetramido Compounds and New Metal Insertion Process. United States, 2004, US 2004/0167329.

(18)   Wietelmann, U.; Lischka, U.; Schade, K.; Panitz, J.-C.: Method for the production of hydrogen bis(chelato)borates and alkali metal bis(chelato)borates. Chemetall G.m.b.H., Germany . 2002; pp 28 pp.

(19)   Sun, J.; MacFarlane, D. R.; Forsyth, M.: Synthesis and properties of ambient temperature molten salts based on the quaternary ammonium ion. *Ionics* **1997**, *3*, 356-362.

(20)   Zhang, X.; Kostecki, R.; Richardson, T. J.; Pugh, J. K.; N., R. J. P.: *J. Electrochem. Soc.* **2001**, *148*, A1341-A1345.

(21)   Xu, K.; Angell, C. A.: High Anodic Stability of a New Electrolyte Solvent: Unsymmetric Noncyclic Aliphatic Sulfone. *Journal of the Electrochemical Society* **1998**, *145*, L70-L72.

(22)   Xu, K.; Angell, C. A.: Sulfone-Based Electrolytes for Lithium-Ion Batteries. *Journal of the Electrochemical Society* **2002**, *149*, A920-A926.

(23)   Sun, X. G.; Angell, C. A.: New Sulfone Electrolytes for Rechargeable Lithium Batteries Part I. Oligoether Containing Sulfones. *Electrochem. Commun.* **2005**, *7*, 261-266.

(24)   Sun, X. G.; Angell, C. A.: Doped sulfone electrolytes for high voltage Li-ion cell applications. *Electrochemistry Communications* **2009**, *11*, 1418-1421.

(25)   Xu, K.; Lee, U.; Zhang, S. S.; Jow, T. R.: GraphiteÕElectrolyte Interface Formed in LiBOB-Based Electrolytes II. Potential Dependence of Surface Chemistry on Graphitic Anodes. *J. of Electrochem. Soc.* **2004**, *151*, A2106-A2112.

(26)   Andersson, A. M.; Herstedt, M.; Bishop, A. G.; Edstrom, K.: The Influence of Lithium Salt on the Interfacial Reactions Controlling the Thermal Stability of Graphite Anodes. *Electrochim. Acta* **2002**, *47*, 1885.

(27)   Liao, C.; Han, K. S.; Baggetto, L.; Hillesheim, D. A.; Custelcean, R.; Lee, E. S.; Guo, B. K.; Bi, Z. H.; Jiang, D. E.; Veith, G. M.; Hagaman, E. W.; Brown, G. M.; Bridges, C.; Paranthaman, M. P.; Manthiram, A.; Dai, S.; Sun, X. G.: Synthesis and Characterization of Lithium Bis(fluoromalonato)borate (LiBFMB) for Lithium Ion Battery Applications. *Adv. Energy Mater.* **2014**, DOI: 10.1002/aenm.201301368.

(28)   Zheng, H. H.; Liu, G.; Battaglia, V.: Film-Forming Properties of Propylene Carbonate in the Presence of a Quaternary Ammonium Ionic Liquid on Natural Graphite Anode. *Journal of Physical Chemistry C* **2010**, *114*, 6182-6189.

(29)   Liao, C.; Shao, N.; Han, K. S.; Sun, X.-G.; Jiang, D. E.; Hagaman, E. W.; Dai, S.: Physicochemical properties of imidazolium-derived ionic liquids with different C-2 substitutions. *Physical Chemistry Chemical Physics* **2011**, *13*, 21503-21510.

(30)   Sugimoto, T.; Kikuta, M.; Ishiko, E.; Kono, M.; Ishikawa, M.: Ionic liquid electrolytes compatible with graphitized carbon negative without additive and their effects on interfacial properties. *J. of Power Sources* **2008**, *183*, 436-440.

(31)   Sugimoto, T. A., Yosuke; Handa, Norihisa; Yamagata, Masaki; Kono, Michiyuki; Kikuta, Manabu; Ishiko, Eriko; Ishikawa, Masashi: Effects of organic additives on lithium insertion/extraction for graphite electrode in ionic liquid electrolytes based on bis(fluorosulfonyl)imide. *Electrochemistry (Tokyo, Japan)* **2009**, *77*, 696-698.

(32)   Seki, S.; Kobayashi, Y.; Miyashiro, H.; Ohno, Y.; Mita, Y.; Terada, N.; Charest, P.; Guerfi, A.; Zaghib, K.: Compatibility of N-Methyl-N-propylpyrrolidinium Cation Room-Temperature Ionic Liquid Electrolytes and Graphite Electrodes. *Journal of Physical Chemistry C* **2008**, *112*, 16708-16713.

(33)   Han, H. B.; Liu, K.; Feng, S. W.; Zhou, S. S.; Feng, W. F.; Nie, J.; Li, H.; Huang, X. J.; Matsumoto, H.; Armand, M.; Zhou, Z. B.: Ionic liquid electrolytes based on multi-methoxyethyl substituted ammoniums and perfluorinated sulfonimides: Preparation, characterization, and properties. *Electrochimica Acta* **2010**, *55*, 7134-7144.

Table of Content
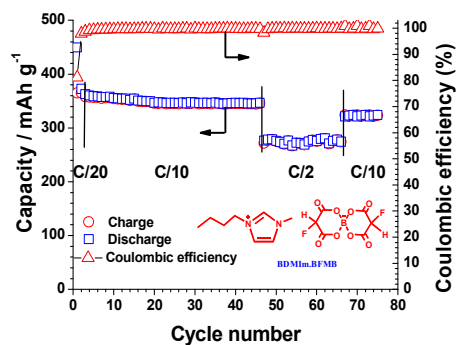
New ionic liquid BDMIm.BFMB is synthesized and used as an additive (5 wt%) in 1.0M $LiPF_6$/PC electrolyte to support reversible charge/discharge in graphite half-cell.